Annular Pressure Reduction During Primary Cementing

Desheng Zhou
College of Petroleum Engineering,
Xian Petroleum University,
Xian, Shanxi 710065, China
e-mail: Desheng@xsyu.edu.cn

Andrew K. Wojtanowicz
Craft and Hawkins Department
Petroleum of Engineering,
Louisiana State University,
3516 CEBA,
Baton Rouge, LA 70803
e-mail: awojtan@lsu.edu

Annular pressure reduction during cementing is a major factor causing annular gas flow. It has been widely accepted and proven experimentally that the pressure reduction phenomenon results from the shear stress opposing downward motion of slurry undergoing volume reduction. The models that have been proposed to describe this process are based on the gel strength and shear stress developments in time and ignore system compressibility. They explain the pressure reduction process observed in the lab where compressibility of the system is very small. However, the models cannot explain the pressure reduction patterns observed on the field where compressibility is significant and the time-dependent effects of cement slurry volume loss significantly contributes to the process. The paper presents a mathematical model combining the effects of gel strength, volume reduction, and compressibility of cement slurry to describe pressure loss in the annular cement column. Results from the model, shown in the paper, compare very well with the data from the laboratory and field tests. Also, the simulated results explain discrepancies between the pressure loss patterns observed in the lab and field tests. [DOI: 10.1115/1.4004809]

Keywords: primary cementing, annular pressure reduction, gel strength model, compressibility model

Introduction

Annular and interzonal gas migration at wells is a major problem of well integrity loss after cement placement and sustained casing pressure—later in the well's operation. The gas migration occurs due to two mechanisms: the entry of gas into the cement slurry column—after placement, or poor bonding of the set cement to either pipe or rock surfaces. Gas may enter the cement slurry column when formation pressure exceeds the hydrostatic pressure in the annulus at the depth of invasion. It has been recognized that the early mechanism of invasion is the percolation of gas through the cemented annulus leading to the development of vertical channels in the cement sheath. Early gas migration has proved to be difficulty to predict and, on occasion, extremely dangerous when migration of H_2S-containing gas is an issue. On the other hand, late-time gas migration causes excessive casing pressures that are persistent and costly to repair.

To date, most of the reported research has related the annular gas migration to hydrostatic pressure loss in the cement column caused by two primary factors: volume reduction and cement slurry gelation. Filtration and chemical shrinkage (hydration) are the major mechanisms of the volumetric loss while gelation restricts the downward movement of the slurry needed to compensate the volumetric. As a result, the pressure compensation is not complete resulting in the reduction of pressure. The amount of pressure lost is controlled by the compressibility of the annular slurry. Thus, qualitatively, compressibility, gelation, and volume reduction should all be included in the mathematical model of the primary cementing process.

The purpose of this study is to develop such a model and use the model to explain various patterns of hydrostatic pressure reported from lab and field.

Modeling pressure reduction in cement column—An overview

Many researchers have tested the pressure reduction of cement slurry in lab. The resulting patterns of the bottomhole pressure reduction are of three types—depending on the authors: Tinsley et al. [2], Sabins et al. [3–5], Stewart and Schouten [21], Cheung and Beirute [22], and Levine et al. [23]. Three plots in Fig. 1 summarize schematically the three patterns.

As shown in Fig. 1, pattern 1 has a concave trend; the shape of pattern 2 is convex, while the pattern 3 gives an s-shape. Interestingly, the major difference of the lab tests was the filtration volume.

To model the pressure reduction phenomenon, basic compressibility correlation was first used by Christian et al. [1] in their studying of cement setting with fluid-loss.

$$\Delta p_{de} = \frac{\Delta v_t}{v}\frac{1}{c_{\text{cem}}} \tag{1}$$

where, Δp_{de}, is the pressure reduction in a cement column, v is the total volume, Δv_t is the total volume loss during cement setting, and c_{cem} is the compressibility of the cement slurry.

Tinsley et al. [2] compared their experimental data on pressure reduction with the calculated values based on the slurry compressibility model for the case of no filtration loss, and obtained good match. Also, the basic compressibility model was used as one of the models to predict pressure reduction by other researchers [3–5]. It was asserted that the model only applies to the fluid in a closed system when sections of the whole cement slurry in annulus are separated by bridges. No further analysis has been made on this subject. Moreover, a rough estimation of compressibility effect showed that total volume reduction is generally so large that it should cause a tremendous pressure reduction even in the lab experiments [4].

Bottomhole pressure reduction has been also studied by considering the cement slurry gelation. The basic formula for pressure loss due to cement gel strength in annulus was first presented by Moore [6]

$$\Delta p_{de} = \frac{4\tau_{\text{gel}}L_{\text{cem}}}{d_w - d_o} \tag{2a}$$

$$\frac{dp}{dh} = \rho g - \frac{4\tau_{\text{gel}}}{d_w - d_o} \tag{2b}$$

where Δp_{de} = pressure loss (reduction), τ_{gel} = static gel strength, L_{cem} = cement column height, d_w and d_o = wellbore and casing

Contributed by the Petroleum Division of ASME for publication in the Journal of Energy Resources Technology. Manuscript received March 15, 2007; final manuscript received July 28, 2011; published online September 6, 2011. Assoc. Editor: Ergun Kuru.

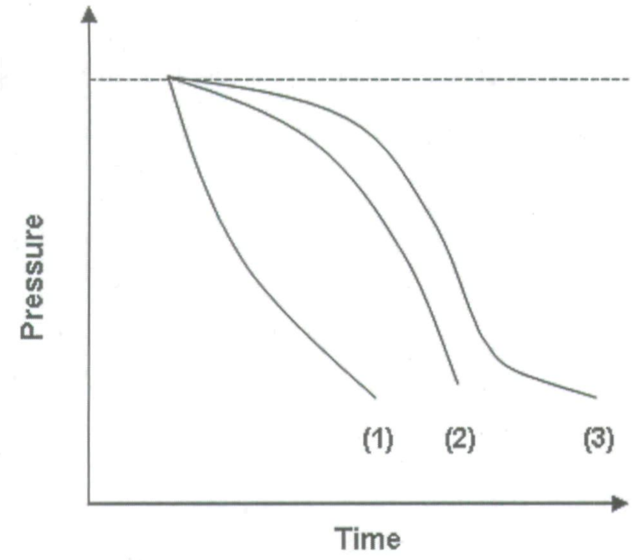

Fig. 1 Patterns of lab-measured pressure reductions during cement setting; pattern 1—[2], pattern 2—[2,21,22], and pattern 3—[2,23]

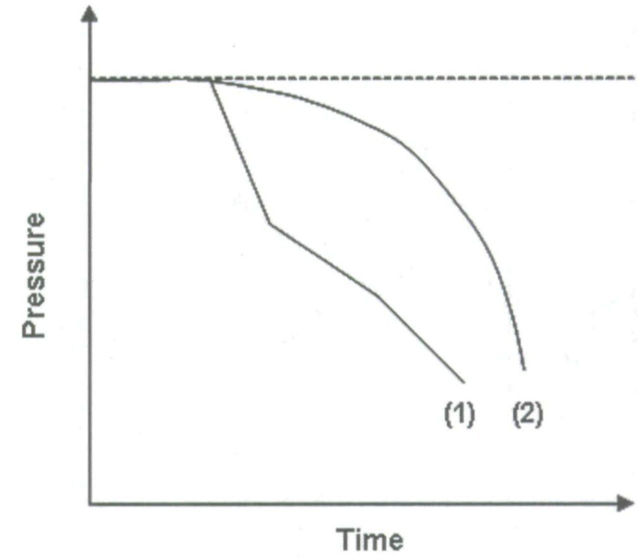

Fig. 2 Pressure reduction in time from models; pattern 1—shear-stress model [7]; pattern 2—compressibility [2], gel-strength [3,4], shear-stress [8,9,18], and Darcy flow [12] models.

outside diameters. And dp/dh = pressure loss gradient along cement column, ρ = cement slurry density.

Sabins et al. [3] used Eq. (2) for pressure analysis during primary cementing. They proposed that Eq. (1) should be used assuming a completely isolated section of the slurry column, Eq. (2) for a free-level slurry, and the actual pressure reduction should be the smaller of the two values from the two formulas. (Eq. (2) was used as a basic model in their other papers [3–5].) Their experimental results verified the validity of Eq. (2) at low filtration rates [3,4]. The tested and calculated pressure reduction patterns resemble pattern 2 in Fig. 1.

Chenevert and Jin [7] proposed a pressure gradient formula using force balance of a free body in the annulus, where cement slurry density, $\rho(t)$, and shear stress, $\tau_s(t)$, vary with time.

$$\frac{dp}{dh} = \rho g - \frac{4\tau_s}{d_w - d_o} \tag{3}$$

Comparing Eq. (3) and Eq. (2*b*), the difference is the shear stress, τ_s, and gel strength, τ_{gel}. Shear stress is the friction and controlled by the pressure reduction value, while gel strength is a property of slurry and is the maximum shear stress at a time.

Using a similar model of Eq. (3), Daccord [8] considered the density term and proposed a density model which was related to slurry compressibility, shrinkage, and time. Also, they used experimental data and presented a model of gel strength versus time as

$$\tau_{\text{gel}}(t) = \tau_{0\text{gel}} e^{(t/T_r)} \tag{4}$$

where, $\tau_{0\text{gel}}$ is the initial gel strength right after cement displacement, τ_{gel} is the gel strength at any elapsed time t after displacement, and T_r is a constant of a slurry.

Prohaska et al. [9] used the same model of Eq. (3) for their pressure reduction analysis. More detailed than the Daccord's work, they studied the depth-dependent (temperature, pressure, and shear rate) behavior of the gel strength evolution.

Four physical properties affecting hydrostatic pressure loss in the column of cement slurry have been identified [10–12]: static gel strength, chemical shrinkage, filtration loss, and permeability of the gelling cement. Using the permeability variation in cement slurry with time, Sabins and Wiggins [12] proposed a model of Darcy's equation for pressure reduction by considering the flow of interstitial water through the permeability to compensate the volume reduction by hydration and fluid-loss.

Again, Sabins and Wiggins [12] proposed that the smaller value from Eq. (2) and from Darcy's equation should be used. They explained that any volume change occurring downhole that could produce a larger pressure loss gradient than that given by the Darcy's equation would produce movement in the whole column of cement including the fluid column above the cement top.

Pressure reduction trends from most of the published models display pattern 2—the convex shape from compressibility model [2], gel strength model [3,4], shear stress model [8,9,18], and Darcy's equation model [12], except the bilinear trend from Chenevert and Jin [7]. However, the pattern of actual pressure reduction in wells measured by Cooke et al. [13,14] is quite different from the convex shape. As shown in Fig. 3, the actual pressure reduction follows the "concave" trend. Chenevert and Jin [7] tried to match Cooke's data with their shear stress model. However, their pressure reduction trend (pattern 1 in Fig. 2) was bilinear instead of "concave".

In conclusion, as shown schematically in Figs. 2 and 3, no mathematical models, so far, could explain the exponential trend (concave trend) of the pressure reduction plots recorded in real wells. Thus, we postulate that the concave pattern results from the system compressibility effect that had not been fully included in the models.

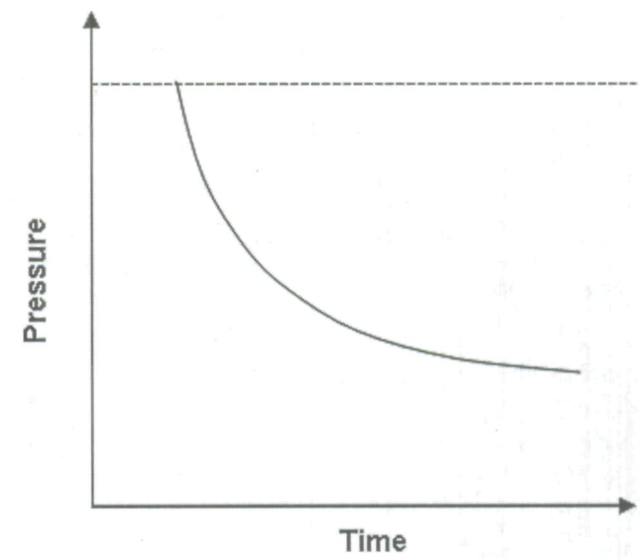

Fig. 3 Field measured pressure reduction [13]

Annular pressure reduction calculation using system compressibility

Physically, pressure reduction at depth in the annular cement slurry column is the result of a shear force along the column that supporting some part (or all) of the column's weight. The shear force comes from shear stresses that oppose downward motion of the column.

The maximum shear stress at any time during slurry setting is the developed gel strength of the slurry at that time. Bottomhole pressure reduction correlates with the shear stress, i.e., larger pressure reduction requires greater shear stress to support the cement column. When shear stress gets its maximum value gel strength, and the shear force is still less than the pressure reduction, the upper column will move down to counteract the pressure reduction.

The compressibility model works for fluid in a container or closed system. During the cement slurry setting, this means no moving down of the slurry.

Compressibility model. From Eq. (1), pressure reduction, Δp_{de}, in an annular element of the cement slurry is caused by volumetric reduction

$$\Delta v_t = c_{\text{cem}} v \Delta p_{de} \tag{5}$$

where, the volumetric reduction, Δv_t, includes the volume reductions due to chemical shrinkage (Δv_{sh}), and filtration loss (Δv_{fil}).

The pressure reduction from the compressibility model of Eq. (5) maybe unrealistically large, which has lead to the conclusion that the compressibility model cannot explain hydrostatic pressure loss in the cement column [4]. However, for an annular element shown in Fig. 4, volumetric loss due to filtration and shrinkage may be compensated by the inward motion of the wellbore wall and the expansion of the casing string due to the pressure reduction of the cement element. Therefore, the two factors should be included in the compressibility.

Another factor affecting the volume reduction is the temperature rise during cement setting. The temperature rise results from the exothermal hydration of cement setting and the geothermal heating from formation. The cement slurry expands with increase of the temperature. The temperature rise will also expand the casing. Only the temperature rise from geothermal heating is considered here as the hydration effect may be included in the result of chemical shrinkage.

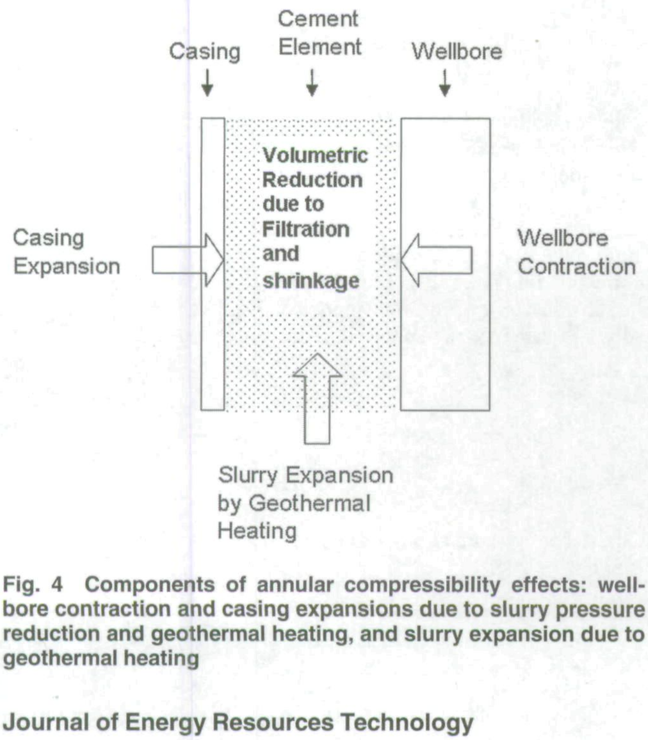

Fig. 4 Components of annular compressibility effects: wellbore contraction and casing expansions due to slurry pressure reduction and geothermal heating, and slurry expansion due to geothermal heating

The total volumetric change, Δv_t, during actual well cementing is

$$\Delta v_t = \Delta v_{\text{fil}} + \Delta v_{sh} - \Delta v_T - \Delta v_{T\text{cas}} - \Delta v_{ww} - \Delta v_{\text{cas}} \tag{6}$$

where, Δv_T and $\Delta v_{T\text{cas}}$ are the slurry and casing expansions due to geothermal heating; Δv_{ww} and Δv_{cas} are the wellbore wall and casing expansions due to pressure reduction. Δv_T, $\Delta v_{T\text{cas}}$, Δv_{ww}, and Δv_{cas} compensate some part of the volume loss (Δv_T and $\Delta v_{T\text{cas}}$) of annular slurry.

Considering all the compensations, as illustrated in Appendices A and B, the Δv_{ww} and Δv_{cas} terms depend on pressure reduction, and are represented by compressibility c_{ww} and c_{cas}. The pressure reduction of a cement column section (Eq. (B11)) is

$$\Delta p_{de} = \frac{\Delta v_{\text{fil}} + \Delta v_{sh} - \Delta v_T - \Delta v_{T\text{cas}}}{v(c_{\text{cem}} + c_{ww} + c_{\text{cas}})} \tag{7}$$

where,

$$\Delta v_T = \frac{1}{4}\pi(d_w^2 - d_o^2)\Delta h \alpha \Delta T$$

$$\Delta v_{T\text{cas}} = 2\pi(1+\mu) r_o^2 \Delta h \beta \Delta T$$

$$c_{ww} = \frac{3 d_w^2}{(d_w^2 - d_o^2) E_f} \tag{8}$$

$$c_{\text{cas}} = \frac{8(1+\mu) r_o^2}{E_{\text{cas}}(d_w^2 - d_o^2)} \left(\frac{(1-\mu)(r_o^2 + r_i^2)}{r_o^2 - r_i^2} - \mu \right) \tag{9}$$

where Δh = slurry section height, μ and E_{cas} = Poisson's ratio and Young's modulus of casing, E_f = Young's modulus of formation rock, α and β = thermal expansion coefficients of slurry and casing, and r_o and r_i = casing inside and outside radii.

The pressure reduction model (Eq. (7)) can also be expressed in terms of volumetric strain, θ, which is the volume change per unit slurry volume

$$\Delta p_{de} = \frac{\theta_{sh} + \theta_{\text{fil}} - \theta_T - \theta_{T\text{cas}}}{c_t} \tag{10}$$

Where: θ_{sh}, θ_{fil}, θ_T, and $\theta_{T\text{cas}}$ are the volumetric strains of shrinkage, filtration, thermal expansion of slurry, and thermal casing expansion, respectively. $c_t = c_{\text{cem}} + c_{ww} + c_{\text{cas}}$, is the total compressibility of the annular slurry system, and

$$\begin{aligned} \theta_T &= \alpha \Delta T \\ \theta_{T\text{cas}} &= 8(1+\mu) r_o^2 \beta \Delta T / (d_w^2 - d_o^2) \end{aligned} \tag{11}$$

Sensitivity analysis of thermal and mechanical effects. Chemical shrinkage is very small, less than 0.3% [11,12], while, during the plastic stage of slurry setting, the volume loss through filtration is of the order of a few percents. Thus, chemical shrinkage part may be ignored for the pressure reduction estimation during the transition time of cement setting.

The relative contributions of the two thermal terms (θ_T and $\theta_{T\text{cas}}$)—slurry expansion and casing expansion due to temperature rise, and two pressure terms (c_{ww} and c_{cas})—casing expansion due to annular pressure reduction and wellbore wall contraction, are studied here.

The well A from Cooke et al. [13,14] is used as well A in the study. The well data are listed in Table 1. To study the effects of casing and wellbore sizes, we also consider well B with the same parameters as those of well A except the casing and wellbore diameters.

Table 1 Well data

Parameters	Well A	Well B
Cased depth, L_{shoe}, m (ft)	2172(8900)	2712(8900)
Bit size, d_w, cm (in.)	20.0(7⅞)	25.08(9.875)
Casing size, d_o, cm (in.)	7.3(⅞)	17.78(7)
Casing size, d_i, cm (in.)	6.2(2.441)	16.17(6.366)
Top of cement, L_{top}, m (ft)	366(1200)	366(1200)
Mud weight, ρ_m, kg/m^3 (lbm/gal)	1222(10.2)	1983(16.6)
Cement slurry, ρ_{cem}, kg/m^3 (lbm/gal)	1983(16.6)	16.7(30)
Temperature rise, T_{rise}, °C (°F)	16.7(30)	$2.07 \times 10^8(3 \times 10^7)$
Casing Young's modulus, E_{cas}, kPa (psi)	$2.07 \times 10^8(3 \times 10^7)$	$1.03 \times 10^7(1.5 \times 10^6)$
Rock Young's modulus, E_t, kPa (psi)	$1.03 \times 10^7(1.5 \times 10^6)$	0.3
Casing Poisson's ration, μ	0.3	$4.95 \times 10^8(2.75 \times 10^8)$
Slurry expansion coefficient, α, °C^{-1}, °F^{-1}	$4.95 \times 10^8(2.75 \times 10^8)$	$1.35 \times 10^7(7.5 \times 10^6)$
Casing expansion coefficient, β, °C^{-1}, °F^{-1}	$1.35 \times 10^7(7.5 \times 10^6)$	

Using Eqs. (8), (9), and (11), θ_T, θ_{Tcas}, c_{ww}, and c_{cas} can be calculated. Table 2 shows the calculated results of the four compensation terms. As shown in Table 2, the effect of casing expansion due to pressure reduction, c_{cas}, is less than one tenth of the well contraction at the same pressure reduction. Also, the compressibility resulting from the wellbore contraction, c_{ww}, is of the same order of magnitude as the slurry compressibility c_{cem}. Therefore, the casing expansion due to annular pressure reduction may be ignored.

The contribution of the four terms to annular pressure reduction was studied by adding each term one by one, as shown in Table 3. A volume reduction rate (chemical shrinkage and filtration) of 1% and temperature increase of 16.67 °C (30°F) were used, and all the other data were in Table 1. As shown in Table 3, according to the basic compression equation (row 3), the pressure drop is very large, 35.5 mPa (5155 psi). Such result would certainly discourage using the basic compressibility model. This is the result without introducing our four compensation terms.

However, this large pressure drop value could be reduced by half when borehole and casing deformations were considered as shown in the forth row of Table 3. Also, the effect of casing expansion due to temperature change of 16.67 °C is small as shown in the fifth row of Table 3. However, as shown in the last row of Table 3, when the temperature expansion of cement slurry (caused by geothermal heating) was considered, a relatively small value of pressure reduction occurred (2661 kPa (386 psi) for well A and 1213 kPa (176 psi) for well B). We might conclude that the two major factors affecting pressure reduction are the wellbore contraction due to pressure reduction and the slurry expansion caused by geothermal heating.

The second conclusion, however, must be treated with caution because, in these calculations, the effect of geothermal heating of the slurry has been simply superimposed on the internal heating effect. We simply assumed here that chemical shrinkage includes the effects of hydration (shrinkage) and expansion due to exothermal reactions, so that the geothermal expansion can be added to the chemical shrinkage.

Average pressure reduction model. The pressure reduction from the compressibility model of Eq. (7) or Eq. (10) varies with depth as geothermal heating and filtration rate depend on depth. To simplify the calculation, average pressure reduction of a cement column is used here. This is correct if the geothermal temperature and filtration rate vary linearly with depth.

$$\Delta\bar{p}_{de} = \frac{1}{2}(\Delta p_{Bde} + \Delta p_{sde}) \tag{12}$$

where Δp_{Bde} = pressure reduction at the bottom of a cement column and Δp_{sde} = pressure reduction on the top of the cement column. $\Delta\bar{p}_{de}$ is the average pressure reduction of the cement column, which is the pressure reduction at the middle of the cement column.

The pressure reduction on the top of the cement column can be treated as zero, if the thickening of drilling mud is ignored. The mud column above cement slurry may flow down easily to compensate the pressure reduction at the top of the slurry.

Generally, filtration volume is either a linear function of the square root of time-for static filtration, or a linear function of time-for dynamic filtration [17]. Dynamic mechanism has been already used to model cement slurry filtration in wells [8,9]. Using dynamic filtration and Darcy's equation over the whole cement column, the total filtration loss of the slurry column is

$$\Delta v_{fil} = \pi d_w D L_{cem} \Delta\bar{p}_{over} t \tag{13}$$

or, in the form of volumetric strain

$$\theta_{fil} = \frac{4 d_w D \Delta\bar{p}_{over} t}{d_w^2 - d_o^2} \tag{14}$$

where, t = elapsed time; D = Darcy's constant; $\Delta\bar{p}_{over}$ = average overbalance pressure of annular pressure over pore pressure at the same depth, which decreases as slurry pressure reducing, and $\Delta\bar{p}_{over} = \bar{p}_{init} - \Delta\bar{p}_{de} - \bar{p}_p$. Where, the average overbalance pressure $\Delta\bar{p}_{over}$, average initial annular pressure $\Delta\bar{p}_{init}$, average pressure reduction $\Delta\bar{p}_{de}$, and average pore pressure $\Delta\bar{p}_p$ are the corresponding pressures at the middle of the cement column.

Substituting the filtration model of Eq. (14) into Eq. (10) and solving for the average pressure reduction, one gets

$$\Delta\bar{p}_{de} = \frac{\dfrac{(\theta_{sh} - \theta_T - \theta_{Tcas})(d_w^2 - d_o^2)}{4 d_w D\, t} + \bar{p}_{init} - \bar{p}_p}{\dfrac{c_t(d_w^2 - d_o^2)}{4 d_w D t} + 1} \tag{15}$$

The slurry pressure at any place, z, and time, t, during cement setting is

$$p(z,t) = p(z)_{init} - \frac{2z}{L_{cem}} \Delta\bar{p}_{de} \tag{16}$$

Table 2 Annular system compressibility

	Well A	Well B
θ_T/Δ_T, °C^{-1} (°F^{-1})	4.95×10^{-4} (2.75×10^{-4})	4.95×10^{-4} (2.75×10^{-4})
θ_{Tcas}/Δ_T, °C^{-1} (°F^{-1})	5.4×10^{-6} (3.00×10^{-6})	3.55×10^{-5} (1.97×10^{-5})
C_{cem}, kPa^{-1} (psi^{-1})	2.81×10^{-7} (1.94×10^{-6})	2.81×10^{-7} (1.94×10^{-6})
C_{ww}, kPa^{-1} (psi^{-1})	3.35×10^{-7} (2.31×10^{-6})	5.83×10^{-7} (4.02×10^{-6})
C_{cas}, kPa^{-1} (psi^{-1})	1.36×10^{-8} (9.35×10^{-8})	9.01×10^{-5} (6.21×10^{-6})

Table 3 Sensitivity analysis of compressibilities

	Well A	Well B
$\theta_{sh}+\theta_{\text{fil}}$	0.01	0.01
ΔT, °C (°F)	16.7(30)	16.7(30)
$\Delta p_{de}=(\theta_{sh}+\theta_{\text{fil}})/C_{\text{cem}}$, kPa (psi)	38,026(5155)	38,026(5155)
$\Delta p_{de}=(\theta_{sh}+\theta_{\text{fil}})/(C_{\text{cem}}+C_{ww}+C_{\text{cas}})$, kPa (psi)	16,031(2325)	10,480(1520)
$\Delta p_{de}=(\theta_{sh}+\theta_{\text{fil}}+\theta_{T\text{cas}})/(C_{\text{cem}}+C_{ww}+C_{\text{cas}})$, kPa (psi)	15,886(2304)	9860(1430)
$\Delta p_{de}=(\theta_{sh}+\theta_{\text{fil}}+\theta_{T\text{cas}}+\theta_T)/(C_{\text{cem}}+C_{ww}+C_{\text{cas}})$, kPa (psi)	2661(386)	1214(176)

We use this average model to analyze the results reported by Cooke et al. [13]. The well A conditions are given in Table 1. We also assume that, during the test, the slurry temperature increase due to geothermal effect was 0.556 °C/h (1°F/h) and the chemical shrinkage rate was 0.018%/h [18]. Average filtration rate was 7.57 l/min (2.0 gal/min) [19], which in this example was converted to unit surface flow rate of 0.00815 $\text{l/m}^2\text{/min}$ (0.0002 gal/ft2/min). The rate was about 5–10 times lower than API drilling mud, 100–200 times lower than API cement fluid-loss for the slurries with fluid-loss additives, and more than 1000 times lower than that without fluid-loss control.

The cement slurry column height $L=2347$ m (8900 ft − 1200 ft = 7700 ft). The initial hydrostatic pressure at the middle of the slurry column is 25.1 mPa (initial hydrostatic pressure at cement bottom = 0.052*10.2*1200 + 0.052*16.6*(8900 − 1200) = 7283 psi, average pressure p_{init} is 7283/2 = 3642 psi = 25.1 mPa). Average pore pressure is 13.3 mPa (0.433*8900/2=1927 psi = 13.3 mPa). The filtration constant $D = 6.8653\times10^{-10}$ m/min/kPa ($1.553\times10^{-8}\ \text{ft}^3/\text{ft}^2/\text{min/psi}$) from Eq. (13). System compressibility $c_t = 6.294\times10^{-7}\ \text{kPa}^{-1}$ ($4.34\times10^{-6}\ \text{psi}^{-1}$) for well A in Table 1.

Cooke et al. [13] measured the pressure reductions at depths of 2668, 2106, 1673, 1459, 1412, and 1108 m (8754, 6909, 5488, 4787, 4632, and 3636 ft). By substituting Eq. (15) into Eq. (16) and solving for the pressures versus time at the same depths, we calculate pressure change versus time, as shown in Fig. 5.

It is evident from Fig. 5 that pressure plots follow an exponential decline pattern. The predicted pressures match the field results measured by Cooke et al. [13].

Depressurized column height calculation using gel strength model

If there is a fluid-loss zone (leak zone) at a certain depth of the slurry column, a "large" volume loss occurs at that spot. This "large" bottom volume loss would cause large pressure reduction at this particular depth and the above cement slurry would move down to fill the gap.

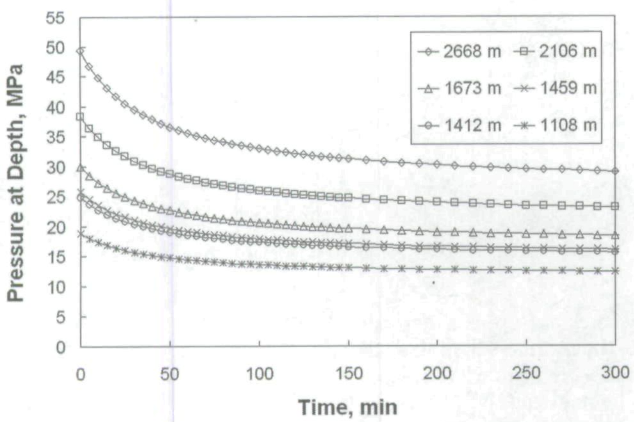

Fig. 5 Comparison of calculated pressures (average compressibility model) with field measured data by Cooke et al. [13]

As slurry gel strength increases with time, the slurry column above the leak zone will finally be held by the developed gel force at a time, and the slurry column will not fall down anymore. After that time, as the gel strength increases further, the gel force on part of the slurry column above the leak zone will be large enough to counteract the bottom pressure reduction. That is, at this time, the large pressure reduction at the leak zone cannot transfer to the top of the slurry column, and can only affect a section of the slurry column from the leak zone upward. The section works as a bridge stopping the pressure variation of its above slurry, and it is called pressure trapped section or depressurized section here. The depressurized section was observed in the field by Haberman et al. [19].

As shown in the plot in Fig. 6, OCD is the annular hydrostatic pressure before slurry setting. OC is the pressure gradient of mud and CD is the pressure gradient of cement slurry before setting. As the initial gel strength is very small, the slurry column would be free to move down in response to the large pressure reduction at the leak zone depth. When gel strength increases to some value, the pressure reduction could not transfer to the top of cement anymore, and part of the pressure reduction at the leak zone is trapped in the section of *BA* with a height of *h*. The pressure gradient in the annulus is changed to OC-CB-BA.

The height of the depressurized section decreases with time as the gel strength increases further. As the slurry gets solid (very strong gel strength), a short section above the leak zone, like a small bridge plug, will hold the above slurry and counteract the bottom pressure reduction.

For a pressure reduction at the leak zone Δp_{leak}, the height of the depressurized column, *h,* is calculated by considering the following force balance in a section of slurry column above the leak zone.

$$\pi\tau_{\text{gel}}(d_o+d_w)h = \pi(d_w^2-d_o^2)\Delta p_{\text{leak}}/4 \tag{17}$$

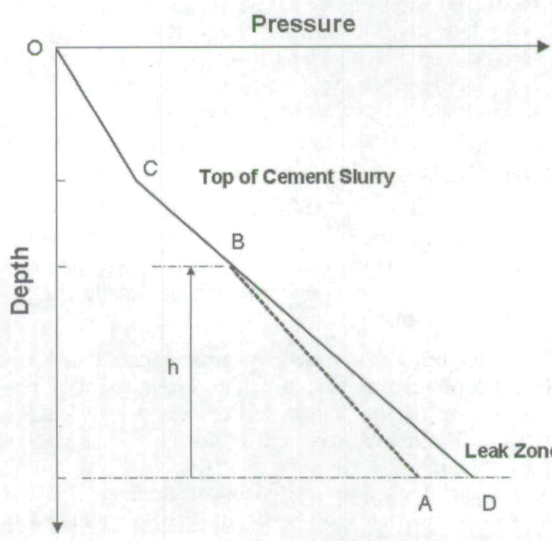

Fig. 6 Depressurized (trapped pressure) slurry column

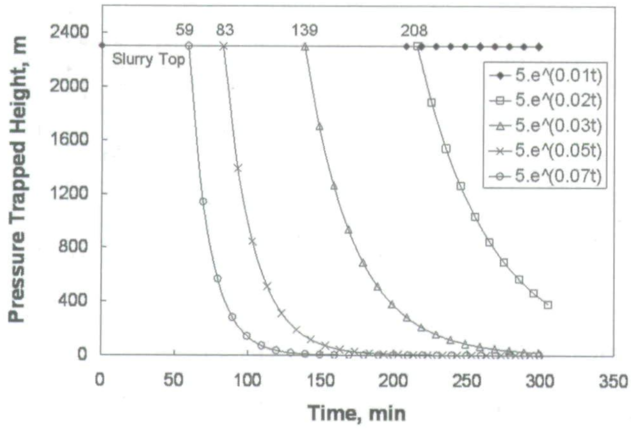

Fig. 7 Calculated depressurized section length versus time for five slurries

Solving Eq. (17) for the depressurized section height h, gives

$$h = \frac{d_w - d_o}{4\tau_{\text{gel}}}\Delta p_{\text{leak}} \tag{18}$$

For a slurry column with trapped pressure section, adding pressure on the top of annular fluid may break the gel strength and make the whole column move down. Cooke et al. [13] observed the phenomenon by adding surface pressure. The pressure in the cement column restored to its original (much greater increase than the added pressure).

As an example of depressurized section calculation, well A data in Table 1 were used. A leak zone was assumed at 2668 m (8754 ft). The cement slurry above the leak zone is 2302 m (8754 ft − 1200 ft = 7554 ft). The hydrostatic pressure at the leak zone before setting is 49.35 mPa (0.052*10.2*1200 + 0.052*16.6*7554 = 7157 psi = 49.35 mPa), and the pore pressure at the place is 26.13 mPa (0.433*8754 = 3790 psi = 26.13 mPa). Assuming the pressure at the leak zone was reduced to the pore pressure there. The pressure reduction, Δp_{leak}, is 23.22 mPa.

Gel strength developing equation (4)) was used in the example. Five cases with $\tau_{0\text{gel}} = 5$ Pa, and constant $1/T_r$ of 0.01, 0.02, 0.03, 0.05, and 0.07 were calculated to study the effect of different slurries.

The depressurized sections were calculated using Eq. (18). The height is measured from the leak zone up to the top of cement slurry. For a calculated height greater than the slurry column (2302 m), the 2303 m was used, which means the pressure reduction was transferred to the top of the cement slurry. For the five slurry cases, shown in Fig. 7, the beginning of pressure trapping occurs after 416, 208, 139, 83, and 59 min, respectively.

As shown in Fig. 7, the height of the depressurized section depends on the developing gel strength of the slurry in the annulus. The depressurized section height decreases with time.

Conclusions

The physical process of hydrostatic pressure loss after cement displacement involves time-dependent effects of gel strength and shear stress. The shear stress results from volume reduction of the slurry and may not reach its maximum value—static gel strength of the slurry at the time.

1. Compressibility model with system compressibility yields a concave pressure reduction pattern during primary cementing, which matches the measured results by Cooke et al. [13,14]. The model may be used for the pressure reduction prediction in wells.
2. The volume reduction from chemical shrinkage and filtration loss is compensated by wellbore wall contraction, casing string expansion, and thermal expansion of cement column due to pressure reduction and geothermal heating. It becomes critical to consider the combination of these effects rather than the cement slurry compressibility alone.
3. If the cement slurry fluid-loss is localized at a high filtration depth (leak zone), pressure reduction may be trapped in the cement column above that depth. The pressure reduction at the leak zone and the height of the depressurized section are controlled by the developed gel strength of cement slurry. The pressure reduction may not reach the cement top.

Acknowledgment

This study was a part of the Louisiana State University research project concerning development of methods and procedures for effective well control in drilling offshore in the Gulf of Mexico, funded by the DOI Mineral Management Services (MMS). The authors would like to express appreciation to MMS for making this work possible. This paper was originally presented as IADC/SPE 59137 at the 2000 IADC/SPE Drilling Conference, held Feb. 23-25 in New Orleans.

Appendix A: Casing expansion

Casing string will expand or contract as the internal and/or external pressure varies. For a uniform symmetrical cylinder, principal stresses and strains are analyzed here. Compressive stresses and strains are assumed as positive and tensile stresses and strains are negative. As long as the deformation of the casing string is in elastic range, stress–strain relation is linear. Therefore, the increases of stress, strain, and pressure are used in the following equations.

Application of the classical elasticity theory for plain strain problem to a casing string of an inner radius r_i and outer radius r_o with external pressure change of Δp_o and internal pressure change of Δp_i. In a cylindrical coordinate system, the radial and tangential (hoop) stresses increases ($\Delta\sigma_r$, $\Delta\sigma\theta$) at any radius r are (Timoshenko and Goodier [20]):

$$\Delta\sigma_r = -\frac{r_i^2\Delta p_i - r_o^2\Delta p_o}{r_o^2 - r_i^2} + \frac{r_i^2 r_o^2(\Delta p_i - \Delta p_o)}{r_o^2 - r_i^2}\left(\frac{1}{r^2}\right)$$
$$\Delta\sigma_\theta = -\frac{r_i^2\Delta p_i - r_o^2\Delta p_o}{r_o^2 - r_i^2} - \frac{r_i^2 r_o^2(\Delta p_i - \Delta p_o)}{r_o^2 - r_i^2}\left(\frac{1}{r^2}\right) \tag{A1}$$

During cement setting, the external pressure drops and the internal pressure is assumed as constant. Eq. (A1) is simplified as

$$\Delta\sigma_r = \frac{r_o^2\Delta p_o}{r_o^2 - r_i^2} - \frac{r_i^2 r_o^2\Delta p_o}{r_o^2 - r_i^2}\left(\frac{1}{r^2}\right)$$
$$\Delta\sigma_\theta = \frac{r_o^2\Delta p_o}{r_o^2 - r_i^2} + \frac{r_i^2 r_o^2\Delta p_o}{r_o^2 - r_i^2}\left(\frac{1}{r^2}\right) \tag{A2}$$

The constitutive relation of any element in the casing string can be expressed as

$$\Delta\varepsilon_r = \beta\,\Delta T + \frac{1}{E_{\text{cas}}}(\Delta\sigma_r - \mu(\Delta\sigma_\theta + \Delta\sigma_z))$$
$$\Delta\varepsilon_\theta = \beta\,\Delta T + \frac{1}{E_{\text{cas}}}(\Delta\sigma_\theta - \mu(\Delta\sigma_r + \Delta\sigma_z))$$
$$\Delta\varepsilon_z = \beta\,\Delta T + \frac{1}{E_{\text{cas}}}(\Delta\sigma_z - \mu(\Delta\sigma_r + \Delta\sigma_\theta)) \tag{A3}$$

where $\Delta\varepsilon_r$, $\Delta\varepsilon\theta$, $\Delta\varepsilon_z$ and $\Delta\sigma_r$, $\Delta\sigma\theta$, $\Delta\sigma_z$ are radial, tangential and vertical principal strains, and stresses. The first term of the right side is the strain increase caused by temperature change. β is the thermal expansion coefficient of the casing string. ΔT is the temperature change of the casing string. The second term on the right side of Eq. (A3) is the well known Hooke's law. E_{cas} is the casing Young's modulus and μ is the casing Poisson's ratio.

For plain strain, ε_z=0, vertical stress is from Eq. (A3)

$$\Delta\sigma_z = -\beta E_{\text{cas}}\Delta T + \mu(\Delta\sigma_r + \Delta\sigma_\theta)) \tag{A4}$$

Tangential strain increase $\Delta\varepsilon\theta$ at radius r determines the displacement increase here from geometric relation of the element.

$$\Delta\varepsilon_\theta = \frac{\Delta u}{r} \tag{A5}$$

Substitution Eq. (A4) into the tangential strain equation Eq. (A3) and substitution Eq. (A3) into Eq. (A5) yields the displacement increase at any radius. For a pressure reduction in the cement slurry Δp_{de} (Δp_o=Δp_{de}) the displacement increase at the outer radius of the casing string Δu_{cas} is

$$\Delta u_{\text{cas}} = (1+\mu)r_o\beta\Delta T + \left(\frac{(1-\mu)(r_o^2+r_i^2)}{r_o^2-r_i^2} - \mu\right)\left(\frac{(1+\mu)r_o}{E_{\text{cas}}}\right)\Delta p_{de} \tag{A6}$$

Appendix B: Pressure reduction

As shown in Fig. 4, the total volumetric change, Δv_t, is

$$\Delta v_t = \Delta v_{\text{fil}} + \Delta v_{sh} - \Delta v_{T\text{cas}} - \Delta v_{ww} - \Delta v_{\text{cas}} \tag{B1}$$

where, $\Delta v_{T\text{cas}}$, Δv_{ww}, and Δv_{cas} are the thermal, wellbore wall and casing expansion, respectively.

Thermal expansion. To estimate the thermal expansion, we can use the definition of thermal expansion coefficient α

$$\alpha = \frac{\Delta v_t}{vdT} \tag{B2}$$

where, v is the cement slurry volume. For a temperature rise of ΔT, the slurry volume expansion is

$$dv_T = \alpha v dT \tag{B3}$$

Assuming the temperature change, ΔT, follows the trend of Horner-type temperature buildup [15]

$$\Delta T = T_f - T_s - \log\frac{\Delta t}{t+\Delta t} \tag{B4}$$

where T_f is the geothermal temperature, T_s is the surface temperature, t and Δt are the total time and elapsed time period. Geothermal temperature at any depth, z, can be calculated from temperature gradient, g_G, or empirical correlation [15].

$$T_f = T_s + g_G z \tag{B5}$$

for shallow wells, or

$$T_f = T_s e^{mz} \tag{B6}$$

for deep wells. Where, m is a constant depending on fields.

Annular system compressibility

The volume of wellbore wall deformation caused by pressure reduction Δp_{de} can be calculated from the displacement of wellbore wall [16].

$$\Delta u_w = \frac{3\Delta p_{de} d_w}{4E_f} \tag{B7}$$

where d_w is the wellbore diameter, E_f is the Young's modulus of the formation. For a wellbore section, Δh, the compensated volume from wellbore wall is

$$\Delta v_{ww} = \pi d_w \Delta u_w \Delta h \tag{B8}$$

Casing expansion comes from geothermal heating of cement slurry and pressure reduction in the slurry. The casing expansion volume is

$$\Delta v_{\text{cas}} = 2\pi r_o \Delta u_{\text{cas}} \Delta h \tag{B9}$$

Where the casing displacement, $\Delta\mu_{\text{cas}}$, is from Eq. (A6).
Substituting Eqs. (B3), (B8), and (B9) into Eq. (B1) and rearranging, one gets

$$\begin{aligned}\Delta v &= \Delta v_{\text{fil}} + \Delta v_{sh} \\ &\frac{1}{4}\pi(d_w^2 - d_o^2)\Delta h(c_{\text{cem}}\Delta p_{de} + \alpha\Delta T) + \frac{3\pi d_w^2}{4E_f}\Delta h \Delta p_{de} \\ &+ 2\pi(1+\mu)r_o^2\Delta h(\beta\Delta T + \frac{1}{E_{\text{cas}}}(\frac{(1-\mu)(r_o^2+r_i^2)}{r_o^2-r_i^2} - \mu)\Delta p_{de})\end{aligned} \tag{B10}$$

Substituting Eq. (B10) into the basic compression equation Eq. (1) and rearranging, one obtains the compressibility model for pressure reduction in annulus.

$$\Delta p_{de} = \frac{\Delta v_{\text{fil}} + \Delta v_{sh} - \Delta v_T - \Delta v_{T\text{cas}}}{v(c_{\text{cem}} + c_{ww} + c_{\text{cas}})} \tag{B11}$$

where

$$\Delta v_T = \frac{1}{4}\pi(d_w^2 - d_o^2)\Delta h \alpha \Delta T$$

$$\Delta v_{T\text{cas}} = 2\pi(1+\mu)r_o^2\Delta h \beta \Delta T$$

$$c_{ww} = \frac{3d_w^2}{(d_w^2 - d_o^2)E_f}$$

$$c_{\text{cas}} = \frac{8(1+\mu)r_o^2}{E_{\text{cas}}(d_w^2 - d_o^2)}\left(\frac{(1-\mu)(r_o^2+r_i^2)}{r_o^2-r_i^2} - \mu\right)$$

The model Eq. (B11) can also be expressed in terms of volumetric strain, θ, which is the volume change per unit slurry volume.

$$\Delta p_{de} = \frac{\theta_{sh} + \theta_{\text{fil}} - \theta_T - \theta_{T\text{cas}}}{c_t} \tag{B12}$$

where θ_{sh}, θ_{fil}, θ_T, and $\theta_{T\text{cas}}$ are the volumetric strains of shrinkage, filtration, thermal expansion of slurry, and thermal casing expansion, respectively. $c_t = c_{\text{cem}} + c_{ww} + c_{\text{cas}}$, is the total compressibility of the annular system, and

$$\begin{aligned}\theta_T &= \alpha\Delta T \\ \theta_{T\text{cas}} &= 8(1+\mu)r_o^2\beta\Delta T/(d_w^2 - d_o^2)\end{aligned} \tag{B13}$$

Average pressure reduction model. The pressure reduction along cement column may vary with depth due to the volumetric loss may be different with place. The control factor is the filtration. Some zones may take more water from the cement slurry. As the slurry at different cement sections may communicate through the permeability of the cement slurry, and a section may fall down if the formed gel strength could not support the pressure reduction below the section, we use average pressure reduction to study the pressure variation of the whole cement column, providing no leak zones.
Average pressure reduction of a cement column, $\Delta\bar{p}_{de}$, is

$$\Delta\bar{p}_{de} = \frac{1}{2}(\Delta p_{Bde} + \Delta p_{Sde}) \tag{B14}$$

where Δp_{Bde} = pressure reduction at the bottom of cement column; Δp_{Sde} = pressure reduction at the top of the cement column, which equals zero as the mud column is easy to fall down to compensate pressure reduction.

Generally, filtration volume is either a linear function of the square root of time-for static filtration, or a linear function of time-for dynamic filtration [17]. Dynamic mechanism has been already used to model slurry filtration [8,9]. Using Darcy's flow equation along the cement column gets the total filtration loss

$$\Delta v_{\text{fil}} = \pi d_w D L \Delta \bar{p}_{\text{over}}\, t \tag{B15}$$

or, in the form of volumetric strain,

$$\theta_{\text{fil}} = \frac{4 d_w D \Delta \bar{p}_{\text{over}}\, t}{d_w^2 - d_o^2} \tag{B16}$$

where, D = Darcy's constant, L = the length of the whole cement column, t = time, $\Delta\bar{p}_{\text{over}}$ = average overbalance pressure, which decreases with slurry pressure reduction

$$\Delta \bar{p}_{\text{over}} = \bar{p}_{\text{init}} - \Delta \bar{p}_{de} - \bar{p}_p \tag{B17}$$

where, $\Delta\bar{p}_{\text{init}}$ = initial average hydrostatic pressure at the middle of cement column, $\Delta\bar{p}_p$ = average pore pressure at the middle of cement column.

Substituting the filtration model Eq. (B16) into Eq. (B12), and solving for the average pressure reduction, one gets

$$\Delta \bar{p}_{de} = \frac{\dfrac{(\theta_{sh} - \theta_T - \theta_{T\text{cas}})(d_w^2 - d_o^2)}{4 d_w D\, t} + \bar{p}_{\text{init}} - \bar{p}_p}{\dfrac{c_t (d_w^2 - d_o^2)}{4 d_w D t} + 1} \tag{B18}$$

The slurry pressure $p(z,t)$ at any place, z, and time, t, during cement setting is

$$p(z,t) = p(z)_{\text{init}} - \frac{2z}{L} \Delta \bar{p}_{de}. \tag{B19}$$

Nomenclature

c = compressibility (volume change per unit volume per kPa), 1/kPa
d = diameter, m
E = Young's modulus, kPa
h = height of depressurized section, m
L = cement slurry length, m
p = pressure at interested depth, kPa
r = radius, m
t = time after cement displacement, minutes
T = temperature, °C
v = volume, m^3
z = length from cement top, m
Δ = increase
Δp_{de} = reduced pressure during cement setting, kPa
Δu = displacement of casing or wellbore wall, mm
μ = Poisson's ratio
α, β = thermal expansion coefficient, 1/°C
ε = strain
θ = volumetric strain (volume change per unit volume), %
ρ = density or equivalent mud density, kg/m^3
σ = Stress, kPa
$_s$ = shear stress, kPa
τ_{gel} = static gel stress, kPa

Subscripts

cas = casing string
cem = cement slurry
f = formation
fil = filtration
i = inside casing
init = initial
o = outside casing
s = surface
sh = shrinkage
T = thermal
t = total
w, ww = wellbore wall

References

[1] Christian, W. W., Chatterji, J., and Ostroot, G. W., 1976, "Gas Leakage in Primary Cementing - A Field Study and Laboratory Investigation," JPT, **28**(11), pp. 1361–1369.
[2] Tinsley, J. M., Miller, E. C., Sabins, F. L., and Sutton, D. L., 1980, "Study of Factors Causing Annular Gas Flow Following Primary Cementing," JPT, **32**(8), pp. 1427–1437.
[3] Sabins, F. L., Tinsley, J. M., and Sutton, D. L., 1982, "Transition Time of Cement Slurries Between the Fluid and Set States," SPEJ, **22**(6), pp. 875–882.
[4] Sabins, F. L., and Sutton, D. L., 1986, "The Relationship of Thickening Time, Gel Strength, and Compressive Strength of Oilwell Cements," SPEPE, **1**(2), pp. 143–152.
[5] Sutton, D. L., Paul, R., and Sabins, F., 1984, "New Evaluation for Annular Gas-Flow Potential," Oil Gas J., **82**(51), pp. 109–112.
[6] Moore, P., *Drilling Practices Manual* (Petroleum Publishing Co., Tulsa, 1974).
[7] Chenevert, M. E., and Jin, L., 1989, "Model for Predicting Wellbore Pressures in Cement Columns," 64th Annual Technical Conference and Exhibition of the SPE, San Antonio, TX, Oct. 8–11, SPE Paper No. 19521.
[8] Daccord, G., 1991, "Cement Slurry Behavior During Hydration and Consequences for Oil-Well Cementing," International Workshop on Hydration and Setting, Dijon, France, July.
[9] Prohaska, M., Ogbe, D. O., and Economides, M. J., 1993, "Determining Wellbore Pressure in Cement Slurry Columns," Western Regional Meeting, Anchorage, Alaska, May 26–28, SPE Paper No. 26070.
[10] Sutton, D. L., and Ravi, K. M., "New Method for Determining Downhole Properties that Affect Gas Migration and Annular Sealing," 64th Annual Technical Conference and Exhibition of the SPE, San Antonio, TX, Oct. 8–11, SPE Paper No. 19520.
[11] Sabins, F. L., and Sutton, D. L., 1991, "Interrelationship Between Critical Cement Properties and Volume Changes During Cement Setting," SPEDE, **6**(2), pp. 88–94.
[12] Sabins, F. L., and Wiggins, M. L., 1997, "Parametric Study of Gas Entry Into Cemented Wellbores," SPEDC, **12**(3), pp. 180–187.
[13] Cooke, C. E., Kluck, M. P., and Medrano, R., 1983, "Field Measurements of Annular Pressure and Temperature During Primary Cementing," JPT, **35**(8), pp. 1429–1438.
[14] Cooke, C. E., Kluck, M. P., Medrano, R., 1984, "Annular Pressure and Temperature Measurements Diagnose Cementing Operations," JPT, **36**(12), pp. 2181–2186.
[15] Bassiouni, Z., 1994, *Theory, Measurement, and Interpretation of Well logs* (SPE Textbook Series), Society of Petroleum Engineers, Richardson, Vol. 4.
[16] Zhou, D., and Wojtanowicz, A. K., 2009, "Cement Seal Failure at Casing Shoe in Shallow Marine Sediments," ASME J. Energy Resour. Technol., **131**(2), 023101.
[17] Daccord, G., and Baret, J. F., 1994, "How Fluid Loss Influences Primary Cementing: Literature Review and Methodology," SPEDC, **9**(2), pp. 133–138.
[18] Prohaska, M., Fruhwirth, R., and Economides, M. J., 1995, "Modeling Early-Time Gas Migration Through Cement Slurries," SPEDC, **10**(3), pp. 178–185.
[19] Haberman, J. P., Delestatius, M., Hine, D. G., Daccord, G., and Baret, J. F., 1992, "Downhole Fluid-Loss Measurements From Drilling Fluid and Cement Slurries," JPT, **44**(8), pp. 872–879.
[20] Timoshenko, S. P., and Goodier, J. N., 1961, *Theory of Elasticity*, 3rd ed., McGraw-Hill Book Co., New York.
[21] Stewart, R. B., and Schouten, F. C., 1988, "Gas Invasion and Migration in Cemented Annuli: Causes and Cures," SPEDE, **3**(1), pp. 77–82.
[22] Cheung, P. R., and Beirute, R. M., 1985, "Gas Flow in Cements," JPT, **37**(6), pp. 1041–1048.
[23] Levine, D. C., Thomas, E. W., Bezner, H. P., and Tolle, G. C., 1979, "Annular Gas Flow After Cementing: A Look at Practical Solution," SPE Annual Technical Conference and Exhibition, Las Vegas, Nevada, Sept. 23–26, SPE Paper No. 8255.